A1120, a Nonretinoid RBP4 Antagonist, Inhibits Formation of Cytotoxic Bisretinoids in the Animal Model of Enhanced Retinal Lipofuscinogenesis

Nicoleta Dobri,[1] Qiong Qin,[1] Jian Kong,[1] Kazunori Yamamoto,[1] Zhao Liu,[1] Gennadiy Moiseyev,[2] Jian-xing Ma,[2,3] Rando Allikmets,[1,4] Janet R. Sparrow,[1,4] and Konstantin Petrukhin[1]

PURPOSE. Excessive accumulation of lipofuscin is associated with pathogenesis of atrophic age-related macular degeneration (AMD) and Stargardt disease. Pharmacologic inhibition of the retinol-induced interaction of retinol-binding protein 4 (RBP4) with transthyretin (TTR) in the serum may decrease the uptake of serum retinol to the retina and reduce formation of lipofuscin bisretinoids. We evaluated in vitro and in vivo properties of the new nonretinoid RBP4 antagonist, A1120.

METHODS. RBP4 binding potency, ability to antagonize RBP4-TTR interaction, and compound specificity were analyzed for A1120 and for the prototypic RBP4 antagonist fenretinide. A1120 ability to inhibit RPE65-mediated isomerohydrolase activity was assessed in the RPE microsomes. The in vivo effect of A1120 administration on serum RBP4, visual cycle retinoids, lipofuscin bisretinoids, and retinal visual function was evaluated using a combination of biochemical and electrophysiologic techniques.

RESULTS. In comparison to fenretinide, A1120 did not act as a RARα agonist, while exhibiting superior in vitro potency in RBP4 binding and RBP4-TTR interaction assays. A1120 did not inhibit isomerohydrolase activity in the RPE microsomes. A1120 dosing in mice induced 75% reduction in serum RBP4, which correlated with reduction in visual cycle retinoids and ocular levels of lipofuscin fluorophores. A1120 dosing did not induce changes in kinetics of dark adaptation.

CONCLUSIONS. A1120 significantly reduces accumulation of lipofuscin bisretinoids in the *Abca4*$^{-/-}$ animal model. This activity correlates with reduction in serum RBP4 and visual cycle retinoids confirming the mechanism of action for A1120.

In contrast to fenretinide, A1120 does not act as a RARα agonist indicating a more favorable safety profile for this nonretinoid compound. (*Invest Ophthalmol Vis Sci.* 2013; 54:85–95) DOI:10.1167/iovs.12-10050

Age-related macular degeneration (AMD) is the leading cause of blindness in developed countries. There is no treatment for the most prevalent dry form of AMD.[1] Dry AMD is associated with abnormalities in the RPE, which lies beneath the photoreceptor cells and provides critical metabolic support to these light-sensing cells. RPE dysfunction induces secondary degeneration of photoreceptors in the central part of the retina, called the macula. Experimental, pathophysiologic and clinical imaging data indicate that high levels of lipofuscin may induce degeneration of RPE and the adjacent photoreceptors in atrophic AMD retinas.[2–8] In addition to dry AMD, dramatic accumulation of lipofuscin is the hallmark of Stargardt disease. One well-known component of RPE lipofuscin is a pyridinium bisretinoid, A2E. Formation of A2E and other lipofuscin bisretinoids, such as A2-dihydropyridine-phosphatidylethanolamine (A2-DHP-PE) and all-trans retinol dimer-phosphatidylethanolamine (atRALdi-PE), begins in photoreceptor cells in a nonenzymatic manner and can be considered as a byproduct of the properly functioning visual cycle.[9,10] It was suggested that small molecule drugs that directly inhibit the visual cycle and/or limit ocular availability of all-trans retinol that fuels the visual cycle may reduce the formation of RPE bisretinoids in the retina, and prolong RPE and photoreceptor survival in patients with dry AMD and Stargardt disease.[11–14] Given that the rates of bisretinoid production in the retina seem to depend on the influx of all-trans retinol from serum to the RPE and assuming that RPE retinol uptake depends on serum retinol concentrations, it was suggested that pharmacologic reduction of serum retinol may represent a common treatment strategy for dry AMD and Stargardt disease.[11] Serum retinol is maintained in circulation as a tertiary complex with retinol-binding protein 4 (RBP4) and transthyretin (TTR). In the absence of interaction of RBP4 with TTR, the RBP4-retinol complex is cleared rapidly from circulation due to glomerular filtration. Retinol binding to RBP4 is required for formation of the RBP4-TTR complex; apo-RBP interacts poorly with TTR. A synthetic retinoid drug fenretinide was found to bind with RBP4, displace all-trans retinol from RBP4,[15] and disrupt the retinol-dependent RBP4-TTR interaction.[15,16] Fenretinide was shown to reduce serum retinol,[17] inhibit ocular all-trans retinol uptake, and slow down the visual cycle.[11] Importantly, fenretinide administration reduced bisretinoid production in the animal model of excessive lipofuscin accumulation.[11] However, independent

of its activity as an antagonist of retinol binding to RBP4, fenretinide is an extremely active inducer of apoptosis in many cell types,[18–22] including the RPE,[23] Additionally, fenretinide is reported to stimulate formation of hemangiosarcomas in mice.[24] Moreover, fenretinide is theratogenic,[25,26] which makes its use problematic in Stargardt disease patients of childbearing age. As fenretinide safety profile may be incompatible with long-term dosing in individuals with blinding but nonlife-threatening conditions, identification of new classes of RBP4 antagonists is of significant importance. A1120, a nonretinoid RBP4 ligand, originally was identified in a screen for compounds that may improve insulin sensitivity.[27] However, administration of A1120 did not improve insulin sensitivity, making it an unlikely drug candidate for diabetes treatment. In our study, we confirmed the ability of A1120 to displace retinol from RBP4, disrupt retinol-induced RBP4-TTR interaction, and reduce serum RBP4 levels. In addition, for the first time to our knowledge, we established the ability of A1120 to inhibit bisretinoid accumulation in the $Abca4^{-/-}$ mouse model of excessive lipofuscinogenesis, which justifies additional evaluation of A1120 and its analogues as a potential treatment for dry AMD and Stargardt disease.

METHODS

Chemicals and Reagents

The 2-(4-[2-(trifluoromethyl)phenyl]piperidine-1-carboxamido)benzoic acid (A1120) and all-trans retinol were purchased from Sigma (St. Louis, MO); 5,6,7,8-tetrahydro-5,5,8,8-tetramethyl-2-naphthalenyl-1-propenyl benzoic acid (TTNPB) was purchased from Biomol (Plymouth Meeting, PA). For the use in the time-resolved fluorescence resonance energy transfer (TR-FRET) assay we expressed the maltose binding protein (MBP)-tagged human RBP4 fragment (amino acids 19–201) in the Gold(DE3)pLysS *Escherichia coli* strain (Stratagene, Santa Clara, CA) using the pMAL-c4x vector. The ligand-binding domain of RARα (amino acids 154–462) was cloned into pGEX-6p-3 and GST-tagged protein was expressed in the Gold(DE3)pLysS *E. coli* strain (Stratagene). Recombinant RBP4 and RARα-LBD were purified using the ACTA FPLC system (GE Healthcare, Pittsburgh, PA) equipped with the MBP Trap HP (for MBP-RBP4) or GST Trap HP (for GST-RARα–LBD) columns. Untagged human RBP4 purchased from Fitzgerald Industries International (Acton, MA) was used in binding experiments. Human TTR was purchased from Calbiochem (San Diego, CA). SRC2-2 peptide, Biotin-Ahx(aminohexanoic acid)-CPSSHSSLTERHKILHRLLQEGSPS-CONH$_2$, was synthesized at CHI Scientific, Inc. (Maynard, MA).

Scintillation Proximity RBP4 Binding Assay

Untagged human RBP4 was biotinylated using the EZ-Link Sulfo-NHS-LC-Biotinylation kit from Pierce (Rockford, IL) following the manufacturer's recommendations. Binding experiments were performed in a final assay volume of 100 μL per well in SPA buffer (1 × PBS, pH 7.4, 1 mM EDTA, 0.1% BSA, 0.5% CHAPS). The reaction mix contained 10 nM ^{3}H-retinol (48.7Ci/mmol; PerkinElmer, Waltham, MA), 0.3 mg/well Streptavidin-PVT beads, 50 nM biotinylated RBP4. Nonspecific binding was determined in the presence of 20 μM of unlabeled retinol. Radiocounts were measured using a TopCount NXT counter (Packard Instrument Company, Meriden, CT) following overnight incubation at 4°C.

TR-FRET Assay for Retinol-Induced RBP4-TTR Interaction

Bacterially expressed MBP-RBP4 and untagged TTR were used in this assay. TTR was labeled with Eu^{3+} Cryptate-NHS using the HTRF Cryptate labeling kit from CisBio (Bedford, MA) following the

manufacturer's recommendations. TR-FRET assay was performed in a final assay volume of 16 μL per well. The reaction buffer contained 10 mM Tris-HCl pH 7.5, 1 mM DTT, 0.05% NP-40, 0.05% Prionex, 6% glycerol, and 400 mM KF. Each reaction contained 60 nM MBP-RBP4 and 2 nM TTR-Eu along with 26.7 nM of anti-MBP antibody conjugated with d2 (CisBio). TR-FRET signal was measured in the SpectraMax M5e Multimode Plate Reader (Molecular Devices, Sunnyvale, CA) following overnight 4°C incubation. Fluorescence was excited at 337 nm; emission was measured at 668 and 620 nm with 75 μs counting delay. The TR-FRET signal was expressed as the ratio of fluorescence intensity: Flu$_{668}$/Flu$_{620}$ × 10,000.

TR-FRET RARα–SRC2-2 Interaction Assay

Bacterially expressed GST-RARα and synthetic biotinylated SRC2-2 peptide (fragment of the SRC1 co-activator) were used in this assay. The reaction buffer contained 10 mM Tris-HCl pH 7.5, 1 mM DTT, 0.05% NP-40, 0.05% BSA, 6% glycerol, and 100 mM KF. Each reaction contained 7 nM GST-RARα and 100 nM SRC2-2. Detection reagents were 0.75 nM europium-labeled anti-GST monoclonal antibody and 42 nM Streptavidin-XL665 (CisBio). After overnight incubation at +4°C, TR-FRET signal was measured as described in the previous section.

Mammalian Two-Hybrid RARα-NCOR Interaction Assay

Expression constructs were made in the pcDNA5FRT vector (Invitrogen, Carlsbad, CA). VP16-RARα–LBD vector contains the fusion gene encoding VP16 activating domain and a DNA fragment encoding amino acids 154-462 of RARα. The GAL-NCoR construct contained the N-terminal 147 amino acids of GAL4 DNA binding domain fused to the nuclear receptor-interacting fragment of corepressor NCoR (protein fragments bracketed by amino acids 1946–2458). Reporter plasmid pGL4.35 (Promega, Madison, WI) contained a luciferase gene under the control of the basal promoter and 9 upstream GAL4-binding elements. CHO cells were plated at 0.5×10^6 cells/well into 96-well plates and transfected with a 0.028 μg pGL4.35 reporter, and equal amounts (0.136 μg) of GAL4- and VP16-constructs using Fugene transfection reagent (Roche, Mannheim, Germany). At 24 hours post-transfection, cells were lysed and assayed for luciferase activity using a Bright-Glo Luciferase Assay System (Promega).

Isomerohydrolase Assay

Bovine RPE microsomal fractions were prepared as described.[28] All-trans 11,12-^{3}H-retinol (1 mCi/mL; 45.5 Ci/mmol; American Radiolabeled Chemical, Inc., St. Louis, MO) dried under argon and resuspended in the same volume of N,N-dimethyl formamide was used as the substrate for the isomerohydrolase assay. For each reaction, 30 μg of microsomal protein were added into 200 μL of reaction buffer (10 mM 1,3-bis[tris(hydroxymethyl)-methylamino] propane [BTP], pH 8.0, 100 mM NaCl) containing 0.2 μM of all-trans retinol, 1% BSA, 25 μM of cellular retinaldehyde-binding protein with or without of test compounds added in 2 μL dimethyl sulfoxide (DMSO). The reaction was stopped and retinoids extracted with 300 μL of cold methanol and 300 μL of hexane, and centrifuged at 10,000g for 5 minutes. The generated retinoids were analyzed by normal phase HPLC as described.[28] The peak of each retinoid isomer was identified based on the retention time of retinoid standards. The isomerohydrolase activity was calculated from the area of the 11-cis retinol peak using Radiomatic 610TR software (PerkinElmer) with synthetic 11-cis ^{3}H-retinol as a standard.

Animal Experiments

Protocols were approved by the Institutional Animal Care and Use Committee of Columbia University and complied with guidelines set forth by the ARVO Animal Statement for the Use of Animals in

Ophthalmic and Vision Res. Ten week-old *Abca4* null mutant mice (129/SV × C57BL/6J) bred as described previously,[29,30] were used to study the A1120 effect on bisretinoid accumulation. *Abca4*^{−/−} and control mice were homozygous for the Rpe65-Leu450 polymorphism. *Abca4*^{−/−} and control *Abca4*^{+/+} mice were raised under 12-hour on-off cyclic lighting with an in-cage illuminance of 30 to 50 lux. For long-term oral dosing A1120 was formulated into Purina 5035 rodent chow at Research Diets, Inc. (New Brunswick, NJ) to ensure consistent 30 mg/kg daily oral dosing. Animals were administered the A1120-containing chow for 6 weeks. To test the effect of A1120 on visual cycle retinoids (11-cis retinaldehyde, all-trans retinaldehyde, all-trans retinyl palmitate) wild-type BALB/cJ mice were dosed for 12 days with the A1120-containing chow to ensure 30 mg/kg daily oral dosing. The influence of A1120 on recovery of the rod response after photo-bleaching was studied in the *Abca4*^{−/−} mice (129/SV × C57BL/6J) as well as in 129/SV wild-type animals dosed with A1120 at the daily dose of 30 mg/kg for the period of 6 weeks in *Abca4*^{−/−} mice and 3 weeks in 129/SV wild-type animals.

Serum RBP4 Measurements

Given the excellent correlation between serum RBP4 and serum retinol across wide range of retinol concentrations,[31] and taking into account the absolute correlation between A1120-induced changes in serum RBP4 and serum retinol in mice,[27] we used serum RBP4 a surrogate marker for serum retinol in this study. Blood samples were collected from a tail vein at days 0, 21, and 42 of the A1120 dosing. Whole blood was drawn into a centrifuge tube and was allowed to clot at room temperature for 30 minutes followed by centrifugation at 2000*g* for 15 minutes at +4°C to collect serum. Serum RBP4 was measured using the RBP4 (mouse/rat) dual ELISA kit (Enzo Life Sciences, Farmingdale, NY) following the manufacturer's instructions.

Retinoid Extraction and Analysis

Following euthanasia, posterior eye cups were pooled and homogenized in PBS using a tissue grinder. For bisretinoid analysis an equal volume of a mixture of chloroform and methanol (2:1) was added, and the sample was extracted three times. Bisretinoids were extracted from the eyecups of untreated wild-type mice (20 eyes), vehicle-treated *Abca4*^{−/−} mice (6 eyes), and A1120-treated *Abca4*^{−/−} mice (8 eyes). Eyecups from vehicle-treated wild-type mice were analyzed as 4 pools of 4 to 6 eyes, while 3 eyes per sample were combined for the analysis of vehicle-treated *Abca4*^{−/−} mice and 4 eyes per sample were combined for the analysis of the A1120-treated *Abca4*^{−/−} mice. To remove insoluble material, extracts were filtered through cotton and passed through a reverse phase (C18 Sep-Pak; Millipore, Billerica, MA) cartridge with 0.1% TFA in methanol. After the solvent had been removed by evaporation under argon gas, the extract was dissolved in methanol containing 0.1% trifluoroacetic acid (TFA), for HPLC analysis. For quantification of bisretinoids of RPE lipofuscin, a Waters Alliance 2695 HPLC system was used with an Atlantis dC18 column (4.6 × 150 mm, 3 μm; Waters, Milford, MA) and the following gradient of acetonitrile in water (containing 0.1% TFA): 90% to 100% from 0 to 10 minutes and 100% acetonitrile from 10 to 20 minutes, with a flow rate of 0.8 mL/min with monitoring at 430 nm. The injection volume was 10 μL. Extraction and injection for HPLC were performed under dim red light. Levels of bisretinoid were determined by reference to external standards of HPLC-purified compound. For the analysis of visual cycle retinoids (11-cis retinaldehyde, all-trans retinaldehyde, all-trans retinyl palmitate) eyes were enucleated from light-adapted animals following the 2-hour exposure to the 30 lux light. A total of 16 eyes for each of the A1120-treated and vehicle control groups was used in the analysis. Two eyes from the individual mouse were homogenized in 1 mL of Dulbecco's phosphate-buffered saline containing 4 M hydroxylamine and incubated at ambient temperature for 30 minutes. All-trans retinyl acetate (atRAc) was added to the homogenate as an internal standard after which the mixture was extracted with chloroform (3 × 2 mL). After filtration, the organic layers were combined and dried under argon. The

sample was redissolved in 10 μL hexane and injected into Waters Acquity UPLC-ESI/MS (Waters). Normal phase chromatography was employed using an Acquity UPLC BEH Amide Column (130Å, 1.7 μm, 2.1 × 100 mm; Waters) and solvent elution with hexane (A) and hexane-dioxane-isopropanol (60:36:4, vol/vol/vol; B) with the following gradient of solvent A: 0 to 3 minutes, 99.8%; 3 to 13 minutes, 99.8% to 95%; 13 to 28 minutes, 95% to 80%. The flow rate was 0.5 mL/min. UV absorbance peaks were identified by comparison with external standards of all-trans retinyl palmitate (Sigma-Aldrich, St. Louis, MO), and retinal oximes of all-trans retinol (Sigma-Aldrich) and 11-cis-retinal (a gift from Rosalie Crouch; synthesis and distribution of the reference 11-cis-retinal samples is supported by the National Eye Institute). Identification was confirmed by mass to charge ratio (m/z). The recovery of atRAc was used to calibrate for loss during extraction. Molar quantities per eye were calculated by comparison to standard concentrations determined spectrophotometrically using published extinction coefficients[32] and values were normalized to total sample volumes.

Electroretinography

Mice were dark-adapted overnight before ERG experiments. Mice were anesthetized with ketamine (80 mg/kg) and xylazine (5–10 mg/kg), and pupils were dilated with 1% phenylephrine and 1% cyclopentolate, followed by an exposure to 5000 lux of bleaching light for 2 minutes. Under these conditions, >90% of the rhodopsin is bleached.

The ERG was recorded from the cornea with cotton wick saline electrodes for 50 minutes immediately after bleaching. Subcutaneous 30 gauge needles on the forehead and trunk were used as reference and ground electrodes, respectively. The light stimulus was obtained from a Ganzfeld stimulator having a stroboscope (PS33 Grass Instruments Inc., West Warwick, RI) removed from its housing, and recessed above and behind the head of the mouse. The flash was diffused to cover the Ganzfeld homogeneously. Maximum flash intensity was measured with a calibrated light meter (J16; Tektronics Instruments, Beaverton, OR). Responses were averaged by a Macintosh computer-controlled data acquisition system (PowerLab; AD Instruments, Mountain View, CA) at a frequency of 0.1 Hz.

RESULTS

Comparison of A1120 and Fenretinide in RBP4 Binding Assay

To establish a scintillation proximity binding assay for RBP4 ligands, we first conducted saturation binding experiments using a fixed amount of biotinylated RBP4 immobilized on Streptavidin-PVT beads and increasing concentrations of ^{3}H-retinol (Fig. 1A). Non-specific binding was defined as radioligand binding in the presence of 20 μM all-trans retinol. Nonlinear regression analysis conducted following saturation binding revealed a dissociation constant (K_d) of 62.5 nM. The K_d for retinol binding to RBP4 defined in our saturation binding experiments is in line with two previously reported values, 70[33] and 60[11] nM, while being somewhat different from the two other literature values, 190[34] and 29[27] nM. To compare A1120 and fenretinide potency, we conducted competitive binding experiments with A1120 and fenretinide at the fixed 10 nM concentration of ^{3}H-retinol (Fig. 1B). The average IC_{50} for A1120 defined in five independent experiments was 14.8 nM, while the IC_{50} for fenretinide was determined to be 56 nM.

Characterization of Compounds in the TR-FRET RBP4-TTR Interaction Assay

To compare the ability of A1120 and fenretinide to antagonize retinol-dependent RBP4-TTR interaction, we developed a TR-FRET assay that probes retinol-dependent RBP4-TTR interaction.
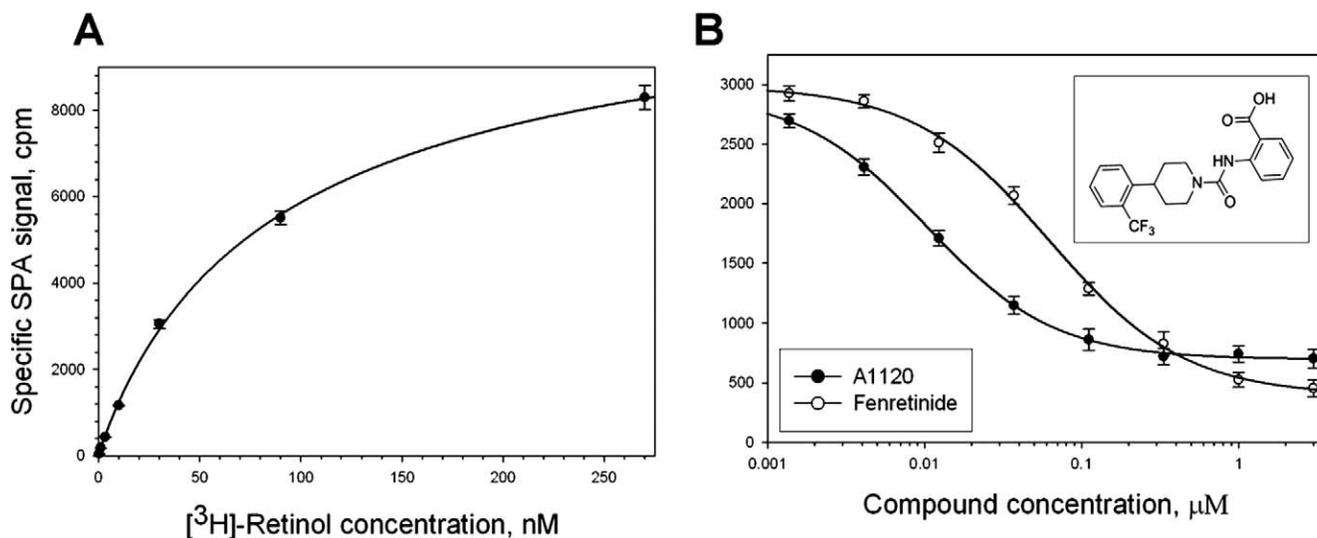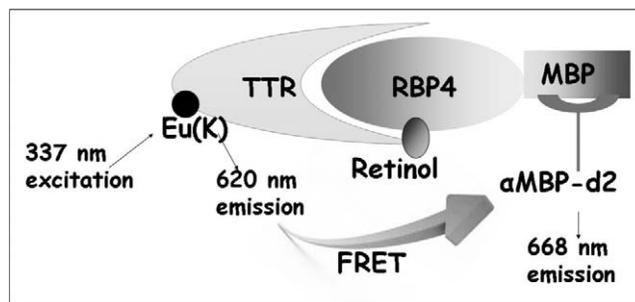
FIGURE 1. Characterization of test compounds in SPA-based RBP4 binding experiments. (**A**) Saturation isotherm for the binding of ^{3}H-retinol to human RBP4. Biotinylated RBP4 (50 nM) was incubated with increasing concentrations of ^{3}H-retinol (0.37–270 nM) in a total volume of 100 µL. Nonspecific binding was assessed in the presence of 20 µM nonradioactive retinol. Presented results are from the representative experiment performed in triplicate. Similar titration data were obtained in two additional experiments. (**B**) Representative isotherms of A1120 and fenretinide binding to human RBP4. ^{3}H-retinol at 10 nM was used as a radioligand. *Upper inset* shows the A1120 structure.

We used *E. coli*-expressed MBP-tagged RBP4 and commercially available TTR labeled directly with Eu^{3+} cryptate along with a d2-conjugated anti-MBP monoclonal antibody to develop this assay (Fig. 2). Retinol-induced RBP4-TTT interaction brings europium in close proximity to the d2 dye, while the 337 nm light excites europium with the following energy transfer to d2, which in turn emits light at 668 nm (Fig. 2). The FRET signal, measured as a 668 nm emission, is normalized using the 620 nm europium emission. The ratiometric nature of the assay normalizes for pipetting and dispensing errors, while homogeneous mode makes reagent changes and washings unnecessary. To determine the optimum concentration of all-trans retinol stimulating the RBP4-TTR interaction, we performed a 12-point retinol titration. We demonstrated that all-trans retinol stimulates RBP4-TTR interaction in a dose-dependent manner (Fig. 3A) with EC_{50} of 308 nM. We compared the ability of A1120 and fenretinide to antagonize retinol-dependent RBP4-TTR interaction by conducting their titrations in the TR-FRET RBP4-TTR interaction assay in the presence of 1 µM retinol. We showed that both compounds are capable of antagonizing retinol-dependent RBP4-TTR interaction (Fig. 3B). It is clear, however, that in the assay conditions A1120 behaves as a much more potent antagonist ($IC_{50} = 155$ nM, $n = 4$, SD = 30) than fenretinide ($IC_{50} = 4.5$ µM, $n = 3$, SD = 0.9).

Assessment of Compound Specificity in the RAR Counter-Screens

It has been suggested that the activity of fenretinide that is associated with its adverse effects may be mediated by its action as a ligand of a nuclear receptor RAR.[18,23,35,36] To develop the counter-screens for comparing A1120 and fenretinide activity as putative RARα ligands we established two assay systems. First, we developed a TR-FRET assay for agonist-induced RARα interaction with transcriptional co-activator SRC1 using the GST-tagged RARα ligand-binding domain (LBD) and a synthetic SRC1 fragment. RARα is a ligand-activated transcription factor; in response to binding of an agonist to its LBD, RARα recruits transcriptional co-activators, such as SRC1.[37] Co-activators, including SRC1,

contain a short conserved LXXLL motifs that is sufficient for binding to a nuclear receptor in an agonist-dependent manner.[37,38] We synthesized a SRC2-2 peptide derived from the SRC1 co-activator (LKEKHKI**L**HR**LL**QDSSSP) which interacts with nuclear receptors in an agonist-dependent manner. Agonist-induced RARα-SRC1 interaction brings to proximity two detector reagents, streptavidin-XL665 and Eu^{3+} cryptate-labeled anti-GST antibody, which generates a FRET signal. Using TTNPB, a control RARα agonist, we confirmed assay performance by documenting dose-dependent increase in TTNBP-induced interaction of SRC2-2 with GST-RARα–LBD (Fig. 4A). After conducting dose titrations for fenretinide and A1120 in this assay, we established that fenretinide was capable of inducing RARα–SRC2-2 interaction confirming that at higher concentrations it can act as an RARα agonist (Fig. 4B). We showed that A1120 does not increase RARα–SRC2-2 interaction appreciably in this assay (Fig. 4B). To investigate the compound activity as potential RAR ligands in a more physiologic cellular context, we established a mammalian two-hybrid assay that probes agonist-sensitive apo-RARα interaction

FIGURE 2. Schematic depiction of the TR-FRET based assay format for characterization of compounds antagonizing retinol-induced RBP4-TTR interaction. MBP-tagged RBP4 bound to the d2-conjugated anti-MBP antibody interacts with europium-labeled TTR in the presence of retinol. Retinol-induced formation of the RBP4-TTR complex brings europium to the close proximity of d2 initiating energy transfer registered as a FRET signal. Compounds antagonizing retinol-dependent RBP4-TTR interaction induce the reduction of FRET signal.
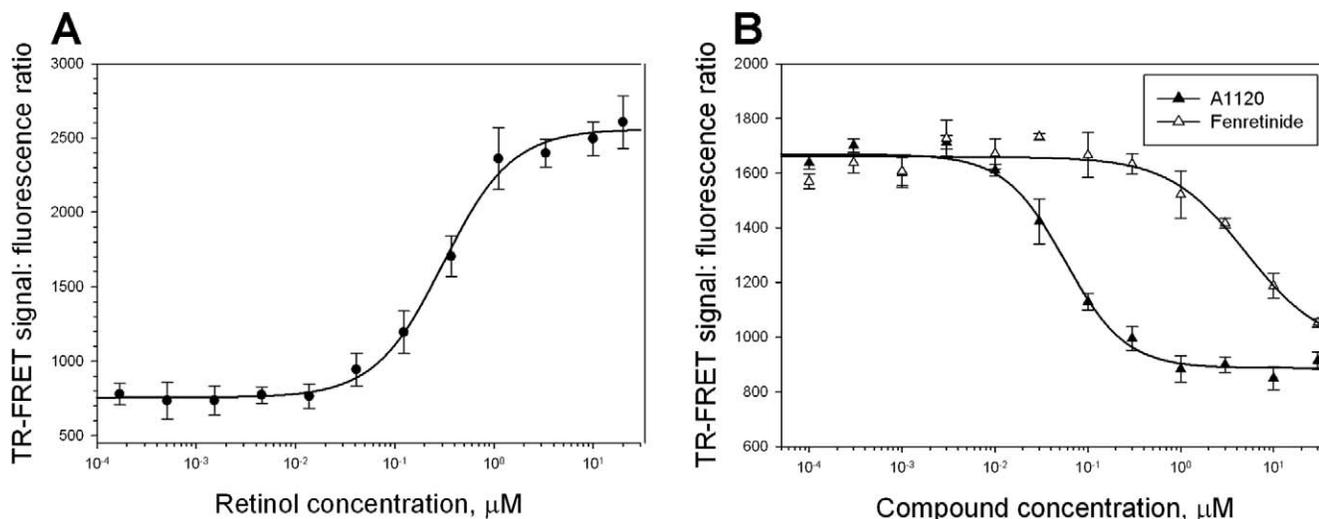
FIGURE 3. Characterization of A1120 and fenretinide in the TR-FRET RBP4-TTR interaction assay. (**A**) Dose-dependent induction of RBP4-TTR interaction by retinol in the TR-FRET assay. (**B**) Antagonist inhibition of retinol-dependent RBP4-TTR interaction by A1120 and fenretinide. In addition to test compounds, retinol at 1 μM was present in the reaction mix. TR-FRET results are shown as fluorescence ratio ($Fl_{668}/Fl_{620} \times 10,000$).

with transcriptional co-repressor NCoR. Similar to many other nuclear receptors, RARα interacts with transcriptional repressors, such as NCoR in the absence of a ligand.[39] Binding of an agonistic ligand induces conformational changes in the ligand-binding domain leading to the release of a co-repressor. Mammalian two-hybrid system is capable of measuring functional interactions between fusion proteins carrying yeast GAL4 DNA binding and viral VP16 transactivation domains. Transient transfection of CHO cells with the GAL4-NCoR and VP16-RARα–LBD constructs along with a reporter plasmid containing nine Gal4 DNA-binding elements upstream of luciferase reporter results in activation of the reporter gene transcription caused by RARα-NCoR interaction. As expected, a control RARα agonist TTNBP dose-dependently inhibited RARα-NCoR interaction (Fig. 4C). Fenretinide was able to inhibit RARα-NCoR interaction in a concentration-dependent manner (Fig. 4D) confirming its ability to act as an RAR agonist. In contrast, A1120 does not exhibit agonistic activity in the mammalian two hybrid RARα-NCoR interaction assay (Fig. 4D).

Correlation between A1120-Induced Serum RBP4 Reduction and Inhibition of Bisretinoid Accumulation in the Retina

To determine whether A1120 has an effect on retinal production of lipofuscin fluorophores we administered the compound at the daily 30 mg/kg dose to *Abca4*^{−/−} mice for a period of 6 weeks. Blood samples collected from the treatment and control groups at baseline, and days 21 and 42 were used to measure serum RBP4 to correlate RBP4 levels with reduction in formation of lipofuscin bisretinoids. As shown in Figure 5, chronic oral administration of A1120 at 30 mg/kg to *Abca4*^{−/−} mice induced a 64% decrease in serum RBP4 level at day 21 and a 75% decrease at day 42. Levels of lipofuscin fluorophores (A2E, A2-DHP-PE, and all-trans retinol dimer-PE) were determined at the end of the 42-day treatment period using quantitative HPLC. Representative chromatogram of lipofuscin fluorophores from eyecups of vehicle-treated *Abca4*^{−/−} mice along with absorbance spectra for the indicated peaks are shown in Figures 6A and 6B. As shown in Figure 6C the levels of bisretinoid accumulation were 3 to 4 times higher in the vehicle-treated *Abca4*^{−/−} mice than in wild-type controls. Administration of A1120 reduces the production of A2E, A2-

DHP-PE, and atRAL di-PE in A1120-treated *Abca4*^{−/−} mice compared to the vehicle-treated *Abca4*^{−/−} animals by approximately 50%. This result demonstrated clearly that A1120 can inhibit in vivo accumulation of toxic lipofuscin bisretinoids in the animal model of enhanced lipofuscinogenesis. We did not note any obvious signs of compound toxicity, such as weight loss or reduction in food consumption during the 6-week-long chronic A1120 dosing.

Effect of A1120 on Isomerohydrolase Activity

It has been suggested in the literature that fenretinide's capacity for A2E reduction may be mediated by its activity as a weak RPE65 inhibitor rather than by its ability to reduce serum RBP4 and retinol.[14] To exclude RPE65 inhibition as a mechanism of action for A1120 we decided to test its capability to inhibit RPE65-mediated isomerohydrolase activity. To assess the inhibitory activity of A1120, we used an in vitro isomer-ohydrolase assay that measures the formation of 11-cis-^{3}H-retinol in bovine RPE microsomes following the addition of all-trans 11,12-^{3}H-retinol, which serves as a precursor of retinyl esters produced by microsomal lecithin retinol acetyltransferase (LRAT). In the absence of test compounds addition of all-trans ^{3}H-retinol to bovine RPE microsomes resulted in formation of radioactive all-trans retinyl esters and production of significant amounts of 11-cis-^{3}H-retinol as shown by HPLC elution profile (Fig. 7A). A1120 added at 200 μM did not inhibit the isomerohydrolase activity (Fig. 7B) while PBN, a positive control,[40] completely inhibited conversion of retinyl esters to 11-cis-^{3}H-retinol by RPE65 (data not shown). These data support the conclusion that direct RPE65 inhibition is not a mechanism by which A1120 inhibits accumulation of lipofus-cin fluorophores.

Effects of A1120 on Levels of Visual Cycle Retinoids

To prove that A1120-induced reduction in serum RBP4 affects the levels of visual cycle retinoids in the eye, we examined retinoid content in the eyecup extracts of wild-type light-adapted mice that were administered orally A1120 at the 30 mg/kg dose for 12 days. The Table shows the steady-state light-adapted levels of 11-cis retinaldehyde, all-trans retinoldehyde, and all-trans retinyl palmitate in eyecup extracts of treated and
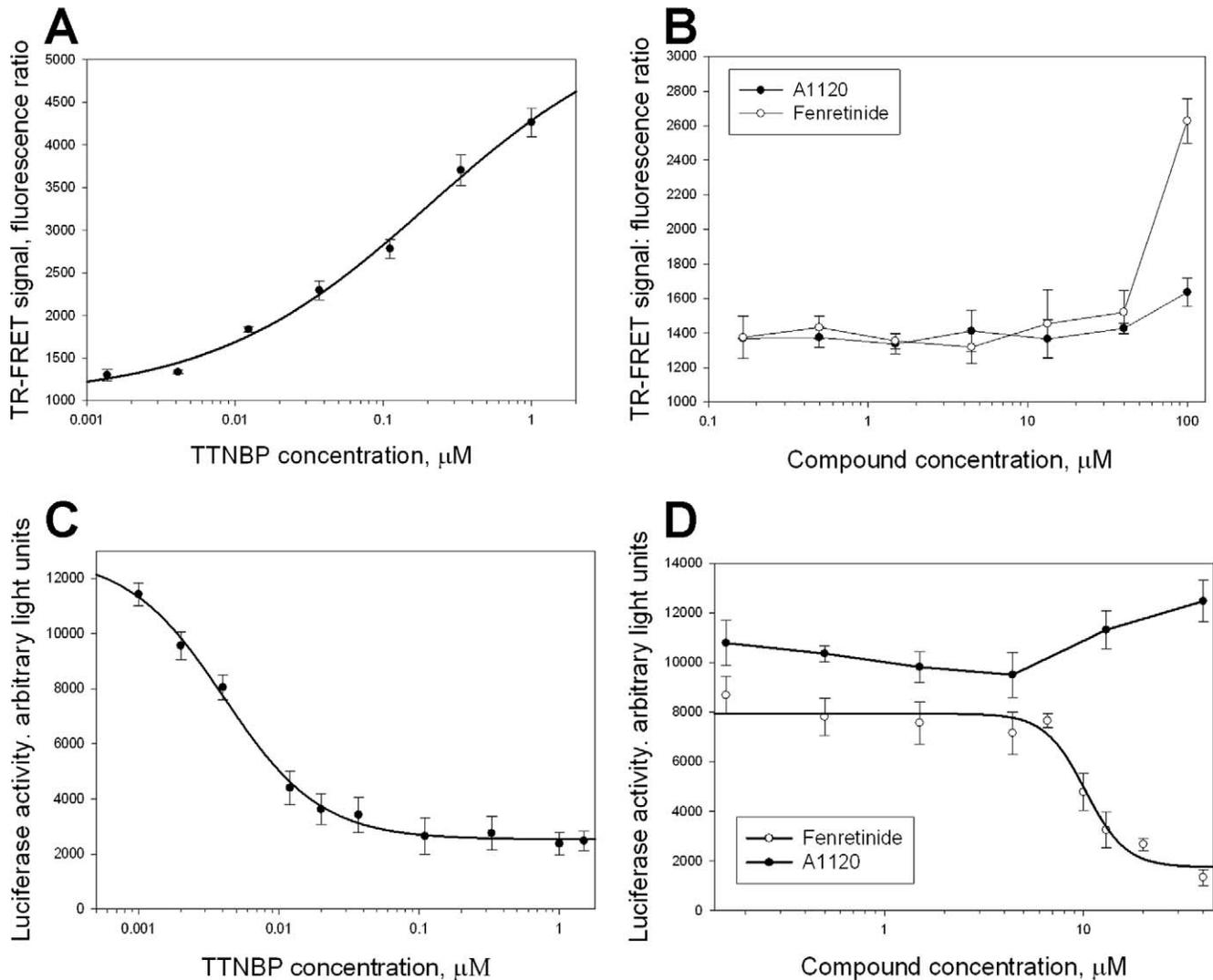
FIGURE 4. Assessment of specificity for A1120 and fenretinide in two RARα assays. Titration of the control RARα agonist, TTNPB, (**A**, **C**) and two test compounds (**B**, **D**) in the TR-FRET RARα-SRC2-2 interaction assay (**A**, **B**), and in the mammalian two-hybrid RARα-NCoR interaction assay (**C**, **D**). TTNBP, as well as fenretinide at higher concentrations, induce conformational changes in the ligand binding domain of RARα that stimulate the release of transcriptional corepressors, such as NCoR, while favoring the interaction with transcriptional co-activators, such as SRC1. In the TR-FRET assay (**A**, **B**) agonist-induced interaction of GST-tagged RARα fragment with biotinylated co-activator peptide, SRC2-2, is registered as a FRET signal generated by energy transfer from europium-labeled anti-GST antibody to Streptavidin-XL665. In the mammalian two-hybrid assay (**C**, **D**) co-expression of GAL4-RARα and VP16-NCoR fragments resulted in induction of luciferase expression from the reporter plasmid containing Gal4 UAS elements due to constitutative RARα-NcoR interaction that brings VP16 activation function to the vicinity of the luciferase promoter. TTNPB (**C**) as well as fenretinide (**D**) induce dose-dependent release of NCoR from RARα, which is registered as a decrease in luciferase expression.

control animals. The 12-day A1120 treatment induced significant (~30%–50%) reduction in 11-cis retinaldehyde and all-trans retinyl palmitate levels, while the effect of the compound on all-trans retinaldehyde was much less pronounced (see Table). These data established the ability of short-term A1120 administration to reduce visual cycle retinoids, and proved the correlation between A1120-induced reduction in serum RBP4 and partial depletion of ocular retinyl palmitate, a storage form of vitamin A in the retina.

Effect of Chronic A1120 Administration on Visual Function and the Recovery of the Rod Photoresponse following Photobleaching

As it has been reported previously that chronic fenretinide administration in *Abca4*⁻/⁻ mice induced a slight delay in

recovery of rod response following exposure to the bleaching light.[11] We decided to assess the effect of A1120 treatment on kinetics of the b-wave amplitude recovery following the photobleaching. Kinetics of the b-wave recovery in A1120- and vehicle-treated *Abca4*⁻/⁻ mice was analyzed before the start of the treatment (Fig. 8A), after 3 weeks of treatment (data not shown), and following the completion of the 6-week dosing regiment (Fig. 8B). We found no statistically significant difference in the rate of b-wave amplitude recovery in A1120- and vehicle-treated *Abca4*⁻/⁻ mice at three time points studied. We extended the analysis of the A1120 effect on dark adaptation and studied the kinetics of the b-wave recovery in wild-type 129 p3/J mice following 3-week A1120 dosing at 30 mg/kg per day. No statistically significant difference in kinetics of the b-wave recovery after photobleaching was found in the groups of A1120- and vehicle-treated wild-type animals (Figs. 8C, 8D). Our data showed that A1120's capacity for reduction
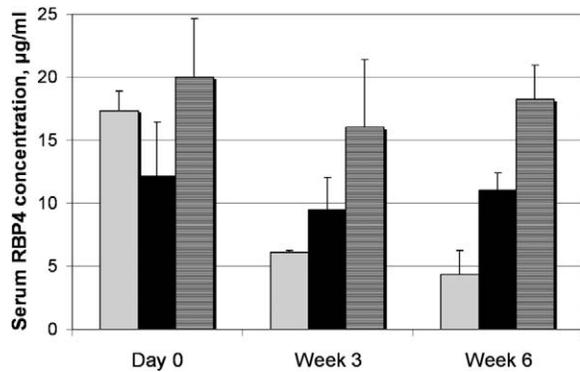
FIGURE 5. Effect of long-term oral A1120 administration on serum RBP4 in *Abca4*^{−/−} mice. Serum RBP4 levels were measured with ELISA test in vehicle-treated wild-type mice (*hatched columns*), vehicle-treated *Abca4*^{−/−} mice (*black columns*), and A1120-treated *Abca4*^{−/−} mice (*gray columns*) at indicated time points. A1120 formulated in a chow was dosed at 30 mg/kg. Compared to day 0, statistically significant 64% RBP4 reduction at week 3 and 75% RBP4 reduction at week 6 is seen in the A1120 treatment group ($P < 0.05$). Changes in RBP4 levels at different time points within the vehicle-treated wild-type and vehicle-treated *Abca4*^{−/−} groups were not statistically significant.

of lipofuscin bisretinoids in the retina is not associated with appreciable suppression of functional recovery of rods after the exposure to the bleaching light.

DISCUSSION

Accumulation of toxic lipofuscin pigment has been implicated in pathogenesis of atrophic AMD and recessive Stargardt disease. It was suggested that formation of cytotoxic lipofuscin bisretinoids occurs in the retina in a nonenzymatic manner and can be considered a byproduct of a properly functioning visual cycle.[9,10] This model assumes that all-trans-retinaldehyde (formed in the outer segments in a light-dependent manner) serves as a direct precursor for A2E synthesis, implying that biogenesis of lipofuscin fluorophores is light-dependent. Recent studies, however, showed no significant difference in lipofuscin and A2E levels between dark- and cyclic light–reared mice,[41] indicating a more complex relationship between the visual cycle and bisretinoid synthesis. While the detailed mechanisms of bisretinoid formation in the retina may require additional elucidation, two pharmacologic classes of compounds have been shown unequivocally to reduce bisretinoid formation in the *Abca4*^{−/−} model of enhanced lipofuscino-
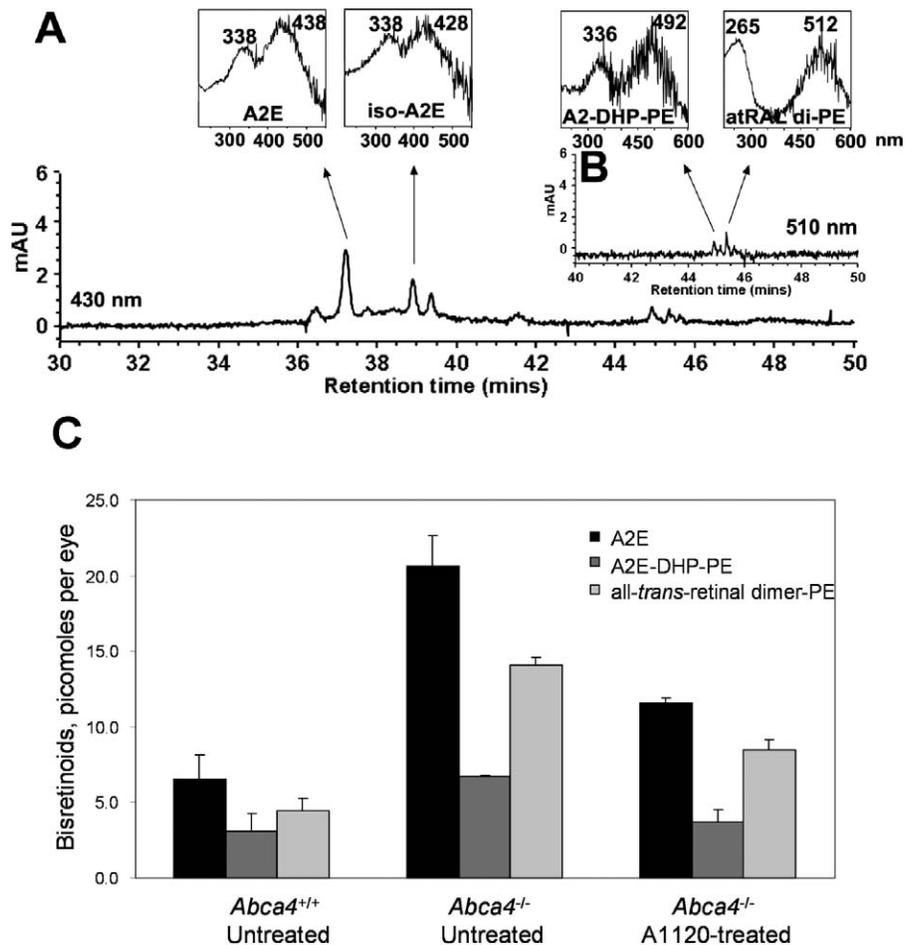
FIGURE 6. Effect of A1120 treatment on the levels of lipofuscin fluorophores in eyes of the *Abca4*^{−/−} mice. Bisretinoids were extracted from the eyecups of vehicle-treated wild-type mice, vehicle-treated *Abca4*^{−/−} mice, and A1120-treated *Abca4*^{−/−} mice after 6 weeks of dosing and analyzed by HPLC. (**A**) The representative reverse phase HPLC chromatogram (monitoring at 430 nm) of an extract from eyecups of A1120-treated *Abca4*^{−/−} mice. *Insets* on the top show UV-visible absorbance spectra of A2E and iso-A2E. (**B**) Chromatographic monitoring at 510 nm, retention time 40 to 50 minutes, for A2-DHP-PE and atRALdi-PE detection, with *insets* on the top showing absorbance UV-visible spectra of A2-DHP-PE and atRALdi-PE. (**C**) Levels of A2E, A2-DHP-PE, and atRALdi-PE in vehicle-treated wild-type mice, vehicle-treated *Abca4*^{−/−} mice, and A1120-treated *Abca4*^{−/−} mice after 6 weeks of dosing showing 45% to 50% reduction in bisretinoid levels in response to A1120 treatment.
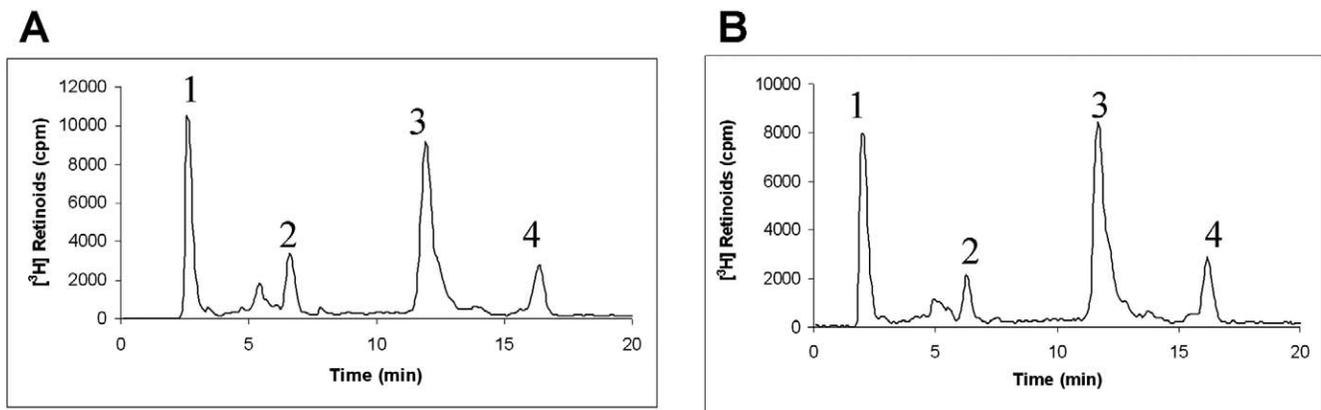
FIGURE 7. Effect of A1120 on isomerohydrolase activity in bovine RPE microsomes. Bovine RPE microsomes (30 µg of protein) were incubated with DMSO (**A**) or 200 µM A1120 (**B**) in the presence of all-trans ^{3}H-retinol (0.2 µM) for 2 hours. The generated retinoids were analyzed by HPLC with *peak 1* representing retinyl ester, *peak 2* representing all-trans retinol, *peak 3* representing 11-cis retinol, and *peak 4* representing all-trans retinol.

genesis. The first class comprises direct inhibitors of key visual cycle enzymes, such as isomerohydrolyze (RPE65) and 11-cis-retinol dehydrogenase. This pharmacologic class is exemplified by isotretinoin,[12] farnesyl isoprenoids,[29] a group of retinyl-amine derivatives,[13,42,43] and a synthetic RPE65 antagonist ACU-4429 of undisclosed structure.[43] The second class of compounds with proven ability to inhibit bisretinoid formation comprises RBP4 antagonists capable of inhibiting retinol-stimulated RBP4-TTR interaction. Until recently, fenretinide was the only representative of this class. It was shown to induce the disruption of the tertiary retinol-RBP4-TTR complex in circulation, with subsequent lowering in serum RBP4 and retinol levels.[11,44] Additionally, it was proven experimentally that fenretinide-induced serum retinol lowering is associated with partial depletion of visual cycle retinoids and accompanied by significant reduction of bisretinoid production in the $Abca4^{-/-}$ model.[11] As fenretinide safety profile may be incompatible with chronic dosing in individuals with atrophic AMD and Stargardt disease, identification of new structural classes of RBP4 antagonists is highly important. A1120, a potent nonretinoid RBP4 antagonist, originally was developed as a potential treatment for diabetes[27] based on the observation that pharmacologic downregulation or genetic ablation of RBP4 enhance insulin sensitivity.[45] However, administration of A1120 to diet-induced obese mice did not improve insulin sensitivity,[27] while re-evaluation of $Rbp4^{-/-}$ phenotype result-ed in a significantly diminished support for RBP4 as a diabetes drug target.[27] Even though A1120 is unlikely to become a diabetes treatment, it may provide a starting point for developing a novel structural class of drugs for atrophic AMD and Stargardt disease. In our study, we conducted a head-to-head comparison of A1120 and fenretinide in a battery of in vitro assays. In competitive binding experiments with RBP4 (Fig. 1) we established that A1120 that demonstrates IC$_{50}$ of 14.8 nM is approximately 4 times more potent than fenretinide (IC$_{50}$ = 56 nM). To compare the ability of A1120 and

fenretinide to antagonize retinol-dependent RBP4-TTR interaction, we conducted compound titrations in the TR-FRET RBP4-TTR interaction assay in the presence of 1 µM retinol. As shown in Figure 3, both compounds are capable of antagonizing retinol-dependent RBP4-TTR interaction. However, under our assay conditions A1120 behaves as a much more potent antagonist (IC$_{50}$ = 155 nM), while significantly higher concentrations of fenretinide are required to antagonize retinol-induced RBP4-TTR interaction (IC$_{50}$ = 4.5 µM). As it has been suggested that fenretinide's adverse effects may be mediated by its action as a ligand of a nuclear receptor RAR,[18,23,35,36] we tested fenretinide along with A1120 in two assays capable of detecting RARα agonistic activity. We established an in vitro TR-FRET assay for agonist-induced RARα interaction with a synthetic fragment of the transcriptional co-activator SRC1. We showed that A1120 does not promote RARα interaction with a SRC1 fragment, STC2-2 peptide, in this assay, which indicates the lack of RARα agonistic activity for A1120 (Fig. 4B). To the contrary, fenretinide was capable of inducing RARα-SRC2-2 interaction, confirming that at higher concentrations it can act as an RARα agonist (Fig. 4B). To assess RARα agonistic activity of test compounds in a more physiologic cellular context, we established a mammalian two-hybrid assay that probes agonist-sensitive apo-RARα interaction with transcriptional co-repressor NCoR. We showed that fenretinide was able to inhibit RARα-NCoR interaction in a concentration-dependent manner (Fig. 4D) confirming its ability to act as an RAR agonist. Consistent with the lack of RARα agonistic activity, A1120 did not affect RARα-NCoR interaction (Fig. 4D). The experiments conducted in two assay formats established clearly that A1120 cannot act as an RARα agonist, indicating that this compound is unlikely to exhibit RAR-mediated adverse effects, which are typical for fenretinide. Attempting to establish the ability of A1120 to inhibit formation of cytotoxic lipofuscin fluorophores (A2E, A2-DHP-PE, and all-trans retinol dimer-PE) in the retina, we administered the compound at the daily 30 mg/kg dose to $Abca4^{-/-}$ mice for a period of 6 weeks. As shown in Figure 6C, administration of A1120 reduces the production of A2E, A2-DHP-PE, and atRAL di-PE in A1120-treated $Abca4^{-/-}$ mice compared to the vehicle-treated $Abca4^{-/-}$ animals by approx-imately 50%. This result demonstrated clearly that A1120 can inhibit in vivo accumulation of lipofuscin bisretinoids in the animal model of enhanced lipofuscinogenesis. Analysis of blood samples collected from the treatment and control groups at different time points revealed 64% decrease in serum RBP4 level at day 21 of compound dosing, while a 75% decrease of

TABLE. Effect of A1120 Treatment on Visual Cycle Retinoids

Treatment Group	11-cis-RAL, pmol/eye	atRAL, pmol/eye	atR Palmitate, pmol/eye
A1120 (8)	124.31 ± 20.81	219.07 ± 37.72	82.55 ± 14.88
Control (8)	232.80 ± 59.91	233.02 ± 43.07	113.72 ± 20.77

Retinoids were extracted from eyes of light-adapted animals and analyzed as described in Materials and Methods. The number of animals per treatment group is shown in parentheses.
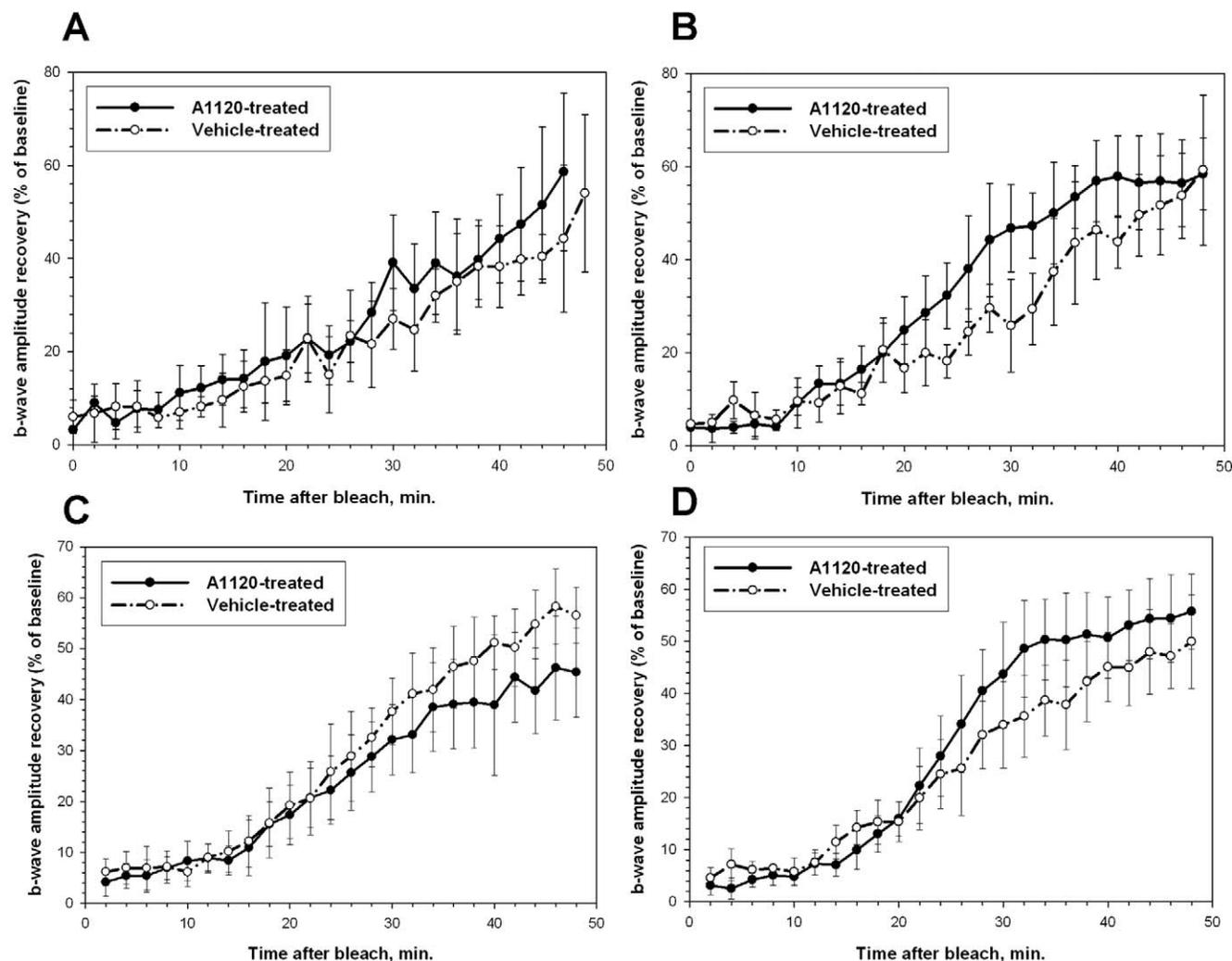
FIGURE 8. Effect of chronic A1120 administration on kinetics of rod b-wave amplitude recovery after photobleaching. Analysis of the recovery of b-wave amplitude after photobleaching was conducted in $Abca4^{-/-}$ (**A**, **B**) and wild-type (**C**, **D**) mice as described in Materials and Methods. (**A**, **C**) Kinetics of b-wave recovery in the A1120-treated and control groups before the start of the compound administration. (**B**, **D**) Kinetics of b-wave recovery in A1120- and vehicle-treated groups after 6 weeks (**B**) and 3 weeks (**D**) of compound administration at the 30 mg/kg per day oral dose.

serum RBP4 in the treatment group was accomplished by day 42 of A1120 administration (Fig. 5). To establish a mechanistic link between serum RBP4 reduction and inhibition of bisretinoid formation, we studied the A1120 effect on visual cycle retinoids. A 12-day A1120 administration in wild-type mice induced significant (~30%–50%) reduction in steady-state light adapted 11-cis retinaldehyde and all-trans retinyl palmitate levels, while the effect on all-trans retinaldehyde was much less pronounced (see Table). These data proved the correlation between A1120-induced reduction in serum RBP4 and partial depletion of ocular retinyl palmitate, a storage form of vitamin A in the retina, and established the ability of A1120 to reduce 11-cis retinal significantly, which may be a direct[41] or indirect precursor of lipofuscin bisretinoids.

As it has been suggested in the literature that fenretinide capacity for A2E reduction may be mediated by its activity as a RPE65 inhibitor rather than by fenretinide-induced reduction in serum RBP4 and retinol,[14] we wanted to exclude inhibition of the isomerohydrolase activity as a mechanism of action for A1120. As shown in Figure 7, A1120 added at 200 μM did not inhibit the isomerohydrolase activity in bovine RPE microsomes, proving that A1120 does not act as an RPE65 inhibitor

in our assay system. The lack of the RPE65 inhibitory activity for A1120 is consistent with the reduction in all-trans retinyl palmitate observed after A1120 dosing (see Table), as it was shown that administration of RPE65 inhibitors has an opposite effect, inducing accumulation of all-trans retinyl esters which occurs downstream of the RPE65 block.[29] Given that conversion of all-trans 11,12-^{3}H-retinol to 11-cis-^{3}H-retinol in bovine RPE microsomes depends on the presence of endogenous LRAT activity, it seems reasonable to conclude that A1120 lacks the ability to inhibit LRAT, which agrees with the recently published observations.[46]

One of the most striking differences between two pharmacologic classes of compounds capable of reducing bisretinoid accumulation in the $Abca4^{-/-}$ mouse model is the degree of visual cycle inhibition associated with bisretinoid reduction. Direct inhibitors of key visual cycle enzymes, such as isotretinoin,[12] farnesyl isoprenoids,[29] and retinylamine,[42] induced profound inhibition of the visual cycle as can be judged by the significant delay in recovery of rod function following exposure to the bleaching light.[12,29,42] In contrast, chronic administration of the RBP4 antagonist fenretinide resulted in a much weaker inhibition of rod response recovery following

exposure to the bleaching light.[11] In our study, we found no difference in kinetics of the b-wave recovery after the photobleach between A1120-treated and control *Abca4*^{−/−} mice after 3 and 6 weeks of compound administration at 30 mg/kg per day (Fig. 8). We extended the analysis of the A1120 effect on dark adaptation and studied the kinetics of the b-wave recovery after the photobleach in wild-type mice following 3 weeks of A1120 dosing. No statistically significant difference in kinetics of the b-wave recovery after photobleaching was found between the groups of A1120- and vehicle-treated wild-type animals (Fig. 8). Our data suggested that A1120's capacity for reduction of lipofuscin bisretinoids in the retina may not be associated with the appreciable suppression of the visual cycle as measured by functional recovery of rods after the exposure to the bleaching light. As was noted previously,[29] the relationship between the extent of visual cycle inhibition and reduction in A2E accumulation is likely to be nonlinear and remains to be understood fully. Our data showing A1120-induced inhibition of the bisretinoid formation without significant suppression of the visual cycle illustrate the complex relationship between the rate of the visual cycle and formation of lipofuscin fluorophores. The lack of appreciable changes in kinetics of dark adaptation in response to A120 treatment in mice may indicate that the clinical use of A1120 derivatives could not be associated with mechanism-based ocular adverse effects (nyctalopia, delayed dark adaptation).

In our current study, we established the correlation between A1120-induced decrease in serum RBP4, partial depletion of certain visual cycle retinoids, and reduced accumulation of lipofuscin bisretinoids in the *Abca4*^{−/−} mouse model, providing rationale for considering A1120 and its derivatives as a potential treatment for atrophic AMD and Stargardt disease. Our study argues in favor of using reduction of serum RBP4 (rather than changes in kinetics of dark adaptation) as a convenient pharmacodynamic marker of compound activity in preclinical and clinical evaluation of this class of molecules. Assuming species-specific differences in non-RBP4–dependent pathways of retinoid supply to the RPE (such as chylomicron delivery[47] and biosynthesis of retinol from β-carotene[48]), the desired levels of RBP4 reduction in patients may differ from levels found to be optimal in the *Abca4*^{−/−} model.

Acknowledgments

References

1. Petrukhin K. New therapeutic targets in atrophic age-related macular degeneration. *Expert Opin Ther Targets*. 2007;11: 625–639.

2. Spaide RF. Fundus autofluorescence and age-related macular degeneration. *Ophthalmology*. 2003;110:392–399.

3. von Ruckmann A, Fitzke FW, Bird AC. Fundus autofluorescence in age-related macular disease imaged with a laser scanning ophthalmoscope. *Invest Ophthalmol Vis Sci*. 1997; 38:478–486.

4. Holz FG, Bellman C, Staudt S, Schutt F, Volcker HE. Fundus autofluorescence and development of geographic atrophy in age-related macular degeneration. *Invest Ophthalmol Vis Sci*. 2001;42:1051–1056.

5. Feeney-Burns L, Hilderbrand ES, Eldridge S. Aging human RPE: morphometric analysis of macular, equatorial, and peripheral cells. *Invest Ophthalmol Vis Sci*. 1984;25:195–200.

6. Sparrow JR, Boulton M. RPE lipofuscin and its role in retinal pathobiology. *Exp Eye Res*. 2005;80:595–606.

7. Delori FC. RPE lipofuscin in ageing and age-related macular degeneration. In: G. Coscas FCP, ed. *Retinal Pigment Epithelium and Macular Disease (Documenta Ophthalmologica)*. Dordrecht, The Netherlands: Kluwer Academic Publishers; 1995:37–45.

8. Dorey CK, Wu G, Ebenstein D, Garsd A, Weiter JJ. Cell loss in the aging retina. Relationship to lipofuscin accumulation and macular degeneration. *Invest Ophthalmol Vis Sci*. 1989;30: 1691–1699.

9. Sparrow JR, Fishkin N, Zhou J, et al. A2E, a byproduct of the visual cycle. *Vision Res*. 2003;43:2983–2990.

10. Sparrow JR, Gregory-Roberts E, Yamamoto K, et al. The bisretinoids of retinal pigment epithelium. *Prog Retin Eye Res*. 2012;31:121–135.

11. Radu RA, Han Y, Bui TV, et al. Reductions in serum vitamin A arrest accumulation of toxic retinal fluorophores: a potential therapy for treatment of lipofuscin-based retinal diseases. *Invest Ophthalmol Vis Sci*. 2005;46:4393–4401.

12. Radu RA, Mata NL, Nusinowitz S, Liu X, Sieving PA, Travis GH. Treatment with isotretinoin inhibits lipofuscin accumulation in a mouse model of recessive Stargardt's macular degeneration. *Proc Natl Acad Sci U S A*. 2003;100:4742–4747.

13. Maeda A, Maeda T, Golczak M, et al. Effects of potent inhibitors of the retinoid cycle on visual function and photoreceptor protection from light damage in mice. *Mol Pharmacol*. 2006;70:1220–1229.

14. Palczewski K. Retinoids for treatment of retinal diseases. *Trends Pharmacol Sci*. 2010;31:284–295.

15. Berni R, Formelli F. In vitro interaction of fenretinide with plasma retinol-binding protein and its functional consequences. *FEBS Lett*. 1992;308:43–45.

16. Schaffer EM, Ritter SJ, Smith JE. N-(4-hydroxyphenyl)retinamide (fenretinide) induces retinol-binding protein secretion from liver and accumulation in the kidneys in rats. *J Nutr*. 1993;123:1497–1503.

17. Adams WR, Smith JE, Green MH. Effects of N-(4-hydroxyphenyl)retinamide on vitamin A metabolism in rats. *Proc Soc Exp Biol Med*. 1995;208:178–185.

18. Fontana JA, Rishi AK. Classical and novel retinoids: their targets in cancer therapy. *Leukemia*. 2002;16:463–472.

19. Holmes WF, Soprano DR, Soprano KJ. Synthetic retinoids as inducers of apoptosis in ovarian carcinoma cell lines. *J Cell Physiol*. 2004;199:317–329.

20. Puduvalli VK, Saito Y, Xu R, Kouraklis GP, Levin VA, Kyritsis AP. Fenretinide activates caspases and induces apoptosis in gliomas. *Clin Cancer Res*. 1999;5:2230–2235.

21. Simeone AM, Ekmekcioglu S, Broemeling LD, Grimm EA, Tari AM. A novel mechanism by which N-(4-hydroxyphenyl)retinamide inhibits breast cancer cell growth: the production of nitric oxide. *Mol Cancer Ther*. 2002;1:1009–1017.

22. Tu Y, Jerry DJ, Pazik B, Smith Schneider S. Sensitivity to DNA damage is a common component of hormone-based strategies for protection of the mammary gland. *Mol Cancer Res*. 2005;3: 435–442.

23. Samuel W, Kutty RK, Nagineni S, Vijayasarathy C, Chandraratna RAS, Wiggert B. N-(4-hydroxyphenyl)retinamide induces apoptosis in human retinal pigment epithelial cells: retinoic acid receptors regulate apoptosis, reactive oxygen species generation, and the expression of heme oxygenase-1 and Gadd153. *J Cell Physiol*. 2006;209:854–865.

24. Cohen SM, Storer RD, Criswell KA, et al. Hemangiosarcoma in rodents: mode-of-action evaluation and human relevance. *Toxicol Sci*. 2009;111:4–18.

25. Decensi A, Zanardi S, Argusti A, Bonanni B, Costa A, Veronesi U. Fenretinide and risk reduction of second breast cancer. *Nat Clin Pract Oncol*. 2007;4:64–65.

26. Turton JA, Willars GB, Haselden JN, Ward SJ, Steele CE, Hicks RM. Comparative teratogenicity of nine retinoids in the rat. *Int J Exp Pathol*. 1992;73:551–563.

27. Motani A, Wang Z, Conn M, et al. Identification and characterization of a non-retinoid ligand for retinol-binding protein 4 which lowers serum retinol-binding protein 4 levels in vivo. *J Biol Chem*. 2009;284:7673–7680.

28. Moiseyev G, Crouch RK, Goletz P, Oatis J Jr, Redmond TM, Ma JX. Retinyl esters are the substrate for isomerohydrolase. *Biochemistry*. 2003;42:2229–2238.

29. Maiti P, Kong J, Kim SR, Sparrow JR, Allikmets R, Rando RR. Small molecule RPE65 antagonists limit the visual cycle and prevent lipofuscin formation. *Biochemistry*. 2006;45:852–860.

30. Kim SR, Fishkin N, Kong J, Nakanishi K, Allikmets R, Sparrow JR. Rpe65 Leu450Met variant is associated with reduced levels of the retinal pigment epithelium lipofuscin fluorophores A2E and iso-A2E. *Proc Natl Acad Sci U S A*. 2004;101:11668–11672.

31. Gamble MV, Ramakrishnan R, Palafox NA, Briand K, Berglund L, Blaner WS. Retinol binding protein as a surrogate measure for serum retinol: studies in vitamin A-deficient children from the Republic of the Marshall Islands. *Am J Clin Nutr*. 2001;73:594–601.

32. Garwin GG, Saari JC. High-performance liquid chromatography analysis of visual cycle retinoids. *Methods Enzymol*. 2000;316:313–324.

33. Noy N, Xu ZJ. Interactions of retinol with binding proteins: implications for the mechanism of uptake by cells. *Biochemistry*. 1990;29:3878–3883.

34. Cogan U, Kopelman M, Mokady S, Shinitzky M. Binding affinities of retinol and related compounds to retinol binding proteins. *Eur J Biochem*. 1976;65:71–78.

35. Sabichi AL, Xu H, Fischer S, et al. Retinoid receptor-dependent and independent biological activities of novel fenretinide analogues and metabolites. *Clin Cancer Res*. 2003;9:4606–4613.

36. Clifford JL, Menter DG, Wang M, Lotan R, Lippman SM. Retinoid receptor-dependent and -independent effects of N-(4-hydroxyphenyl)retinamide in F9 embryonal carcinoma cells. *Cancer Res*. 1999;59:14–18.

37. Lee JW, Lee YC, Na SY, Jung DJ, Lee SK. Transcriptional coregulators of the nuclear receptor superfamily: coactivators and corepressors. *Cell Mol Life Sci*. 2001;58:289–297.

38. Savkur RS, Burris TP. The coactivator LXXLL nuclear receptor recognition motif. *J Pept Res*. 2004;63:207–212.

39. Chen JD, Evans RM. A transcriptional co-repressor that interacts with nuclear hormone receptors. *Nature*. 1995;377:454–457.

40. Mandal MN, Moiseyev GP, Elliott MH, et al. Alpha-phenyl-N-tert-butylnitrone (PBN) prevents light-induced degeneration of the retina by inhibiting RPE65 protein isomerohydrolase activity. *J Biol Chem*. 2011;286:32491–32501.

41. Boyer NP, Higbee D, Currin MB, et al. Lipofuscin and N-retinylidene-N-retinylethanolamine (A2E) accumulate in retinal pigment epithelium in absence of light exposure: their origin is 11-cis-retinal. *J Biol Chem*. 2012;287:22276–22286.

42. Golczak M, Kuksa V, Maeda T, Moise AR, Palczewski K. Positively charged retinoids are potent and selective inhibitors of the trans-cis isomerization in the retinoid (visual) cycle. *Proc Natl Acad Sci U S A*. 2005;102:8162–8167.

43. Kubota R, Boman NL, David R, Mallikaarjun S, Patil S, Birch D. Safety and effect on rod function of ACU-4429, a novel small-molecule visual cycle modulator. *Retina*. 2012;32:183–188.

44. Mata NL, Phan K, Han Y. Assay of retinol-binding protein-transthyretin interaction and techniques to identify competing ligands. *Methods Mol Biol*. 2010;652:209–227.

45. Yang Q, Graham TE, Mody N, et al. Serum retinol binding protein 4 contributes to insulin resistance in obesity and type 2 diabetes. *Nature*. 2005;436:356–362.

46. Amengual J, Golczak M, Palczewski K, von Lintig J. Lecithin: retinol acyltransferase is critical for cellular uptake of vitamin A from serum retinol-binding protein. *J Biol Chem*. 2012;287:24216–24227.

47. Quadro L, Blaner WS, Salchow DJ, et al. Impaired retinal function and vitamin A availability in mice lacking retinol-binding protein. *Embo J*. 1999;18:4633–4644.

48. Chichili GR, Nohr D, Schaffer M, von Lintig J, Biesalski HK. beta-Carotene conversion into vitamin A in human retinal pigment epithelial cells. *Invest Ophthalmol Vis Sci*. 2005;46:3562–3569.